Progress In Electromagnetics Research C, Vol. 19, 163–177, 2011

ENCLOSURE EFFECT ON MICROWAVE POWER AMPLIFIER

J. Dhar and R. K. Arora

MSTD/MSTG/MRSA, Space Applications Centre
ISRO, DOS, Ahmedabad, India

A. Dasgupta

Institute of Radiophysics and Electronics
Calcutta University, India

S. S. Rana

Satish Dhawan Professor, Space Applications Centre
ISRO, DOS, Ahmedabad, India

Abstract—The package design for microwave sub-systems requires adequate knowledge of electromagnetic field distribution inside the package housing. The cavity resonance of the microwave amplifier not only degrades the electrical performance, the feedback through the resonance mode also can cause unwanted oscillation in the frequency band of interest. It may even result in catastrophic failure of the device, wherein the peak oscillating voltage exceeds the device breakdown voltage. Hence, comprehensive analysis of the package effects is one of the prime requirements for stable microwave amplifier design for high-rel applications. This paper describes modeling, analysis of the package and different mitigation techniques used to make stable, resonance free microwave amplifier for a C-band spaceborne SAR payload.

Received 26 November 2010, Accepted 20 January 2011, Scheduled 27 January 2011
Corresponding author: Jolly Dhar (jolly@sac.isro.gov.in).

1. INTRODUCTION

The effect of enclosure on the performance of a C-band power amplifier has been studied by designing an amplifier for the transmit chain of the Transmit-Receive modules, required for an active phase array antenna. The amplifier design is based on the nonlinear model [1] to amplify the input pulsed rf power from 22.5 dBm to 40.8 dBm over the frequency range of 5350 ± 112.5 MHz. The matching topology of the microwave amplifier is selected for minimum coupling effect to provide output power of 12 Watt and suppression of 40 dBc for unwanted frequencies. Since microwave matching circuit consists of lumped and distributed elements, the 2.5D electromagnetic analysis is carried out using Advanced Design Software (ADS) in order to incorporate the coupling effects. Subsequently, this distributed effect is combined with lumped circuit to optimize the overall electrical performance of the circuits. However, the 2.5D electromagnetic analysis does not account for the effect due to the enclosure which is extremely important for the power amplifier design.

2. PRIOR WORK ON MICROWAVE ENCLOSURE

Microwave sub-systems usually consist of several MMIC's and active/passive devices having different package styles [2, 3]. The housing design for high-rel applications is very important as it not only provides necessary mechanical/structural support but also suitable path for heat transfer as well as protection against hostile environments such as temperature, humidity, vibration/shock, EMI/EMC etc. Further, the cavity electrical size increases at high frequency and a number of undesirable parasitic effects degrade the circuit performance. The conductive surface of the enclosure supports several resonant modes and therefore produces the oscillating charges, which in turn induce surface currents on the conductive walls of the package. The methods for eliminating crosstalk due to the above mentioned factors and equivalent circuits for EMI prediction are presented in papers [4–6]. The study on shielding effectiveness of metallic cavities with apertures is discussed in [7–10]. The papers [11, 12] describe the fractional square and rectangular cavity resonator.

3. PACKAGE MODELING AND ANALYSIS

The enclosure for the power amplifier is designed using aluminium alloy "6061-T6". The Kovar carrier plates are used for mounting the alumina substrates as the co-efficient of thermal expansion (CTE) for

both the materials are nearly the same. In an assembled package modeling, the effect of various assembly parts like RF feed-through, packaged devices, isolator, mounting screws etc. is taken into account [13]. The High Frequency Structural Simulator (HFSS) [14] based on Finite Element Method (FEM) is used for the eigen and driven modes study. The following differential equation, also known as Helmholtz wave equation is solved by Finite Element Method:

$$\left(\frac{\partial^2}{\partial x^2}+\frac{\partial^2}{\partial y^2}+\frac{\partial^2}{\partial z^2}+k^2\right)\psi=0, \tag{1}$$

where, ψ is electric or magnetic field.

The FEM breaks the 3D structure into a large number of tetrahedrals. The analysis technique used by HFSS, computes wave patterns (modes) on each port of the structure supported by transmission lines. The 2D field pattern serves as boundary conditions for full 3D structure. Then, the full EM field pattern is computed inside the structure assuming only one mode is excited at a time. The excitation field is expressed as:

$$E(x,y,z,t)=real\left[E(x,y)\exp(jwt-\gamma z)\right] \tag{2}$$

where, $E(x,y)$ is phasor field quantity and γ is complex propagation constant.

The field pattern of a traveling wave is determined by solving Maxwell's equation.

The theoretical resonance frequency of the rectangular cavity is calculated from the given equation:

$$f_{mnp}=\frac{c}{2\pi\sqrt{\mu_r\varepsilon_r}}\sqrt{\left(\frac{m\pi}{a}\right)^2+\left(\frac{n\pi}{b}\right)^2+\left(\frac{p\pi}{c}\right)^2} \tag{3}$$

where "μ_r" is complex relative permeability, "ε_r" is complex relative permittivity, "a" is width, "b" is height and "c" is length.

The eigen mode solver calculates the eigen modes or resonance frequencies of the structure and fields at these resonance frequencies. The driven mode solver calculates S-parameter in terms of incident and reflected signals. Hence, eigen and driven mode analysis is carried out for the package, with width of 40 mm, height of 12 mm and length of 95.2 mm. The results of this analysis for the unassembled and assembled cavity are shown in Table 1, which depicts all the resonance frequency components obtained during cavity analysis. Figures 1 and 2 represents the unassembled cavity and the corresponding coupling for the same. The assembled cavity and its coupling effect are shown in Figures 3 and 4. This represents the corresponding coupling of the package resonant modes due to discontinuities in the package.

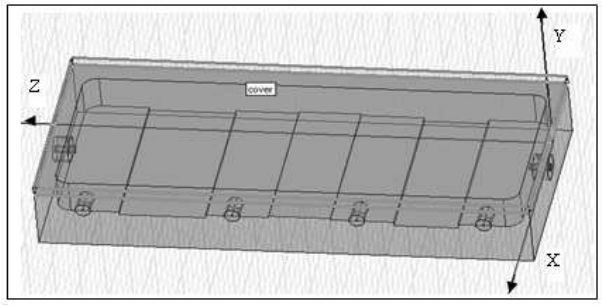

Figure 1. Un-assembled cavity.

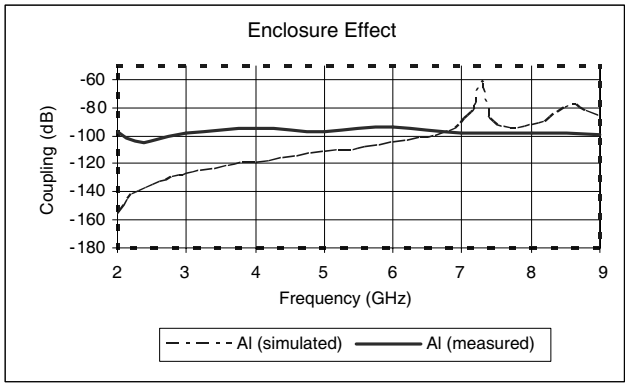

Figure 2. Coupling effect for an un-assembled cavity (Aluminium Alloy).

Table 1. Resonance frequencies of the microwave enclosure.

Different Modes	Un-assembled cavity		Assembled cavity	
	(Theoretical)	(Eigen analysis)	Eigen analysis	Driven Analysis
Mode_1	4.058 GHz	4.050 GHz	3.47 GHz	3.47 GHz
Mode_2	4.898 GHz	4.939 GHz	4.09 GHz	4.05 GHz
Mode_3	6.034 GHz	6.034 GHz	5.17 GHz	5.2 GHz
Mode_4	7.334 GHz	7.260 GHz	7.12 GHz	7.12 GHz
Mode_5	7.664 GHz	7.649 GHz	7.26 GHz	8.20 GHz

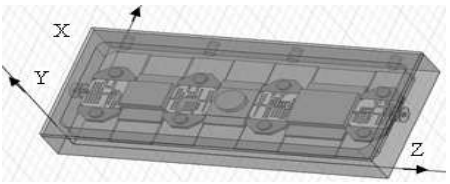

Figure 3. Assembled cavity.

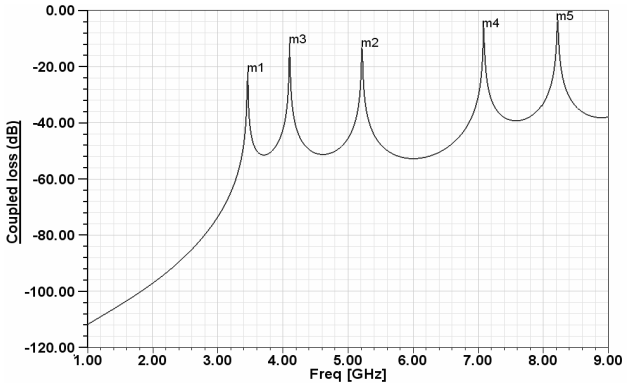

Figure 4. Coupling effect for assembled cavity (Aluminium Alloy).

4. PRACTICAL MITIGATION TECHNIQUES

From the cavity analysis, it is evident that the contribution of cavity resonance is negligible for un-assembled cavity, whereas for assembled cavity, the pass band resonance frequencies are 5.17 GHz and 5.2 GHz respectively. To minimize the effects of these cavity resonances, different mitigation techniques are adopted. These are pre-design and post design mitigation techniques. The pre-design techniques relate to modification of package geometry, material selection and surface treatment. The post design techniques are implemented when packages are already fabricated and new design is not possible due to the impact on cost and schedule. Detail of various mitigation techniques are given below:

4.1. Optimization of Package Geometry

As a pre-design mitigation technique, the theoretical resonance modes for different package geometries are calculated for the un-assembled cavity. The results of package geometry analysis are listed in Table 2.

Table 2. Package geometry based theoretical resonance modes.

Different Mode	Frequency (GHz)				
	Package-1	Package-2	Package-3	Package-4	Package-5
	$a = 29.8$ mm $b = 12$ mm $c = 95.2$ mm	$a = 45$ mm $b = 12$ mm $c = 95.2$ mm	$a = 34$ mm $b = 12$ mm $c = 95.2$ mm	$a = 34$ mm $b = 12$ mm $c = 120$ mm	$a = 34$ mm $b = 12$ mm $c = 34$ mm
Mode 1	5.27	3.68	4.68	4.58	6.24
Mode 2	5.94	4.58	5.42	5.07	9.86
Mode 3	6.90	5.78	6.45	5.79	12.48
Mode 4	8.06	7.13	7.69	6.66	13.95
Mode 5	9.35	7.37	8.96	7.65	15.91

Table 3. Theory and analysis based comparison for width dependent packages.

Package-1					Package-2				
Width (a) = 29.8 mm, Height (b) = 12 mm, Length (c) = 95.2 mm					Width (a) = 45 mm, Height (b) = 12 mm, Length (c) = 95.2 mm				
Analytical	Eigen analysis unassembled		Eigen analysis assembled		Analytical	Eigen analysis unassembled		Eigen analysis assembled	
F (GHz)	F (GHz)	Q	F (GHz)	Q	F (GHz)	F (GHz)	Q	F (GHz)	Q
5.27	5.26	8293	5.29	1301	4.58	4.66	4792	4.50	3227
5.94	5.95	9279	5.85	494.2	5.78	5.46	5354	5.33	3677
6.90	6.89	9914	7.04	150	6.85	6.47	5815	6.45	3985
8.06	7.89	10632	7.86	1533	7.37	7.62	6310	7.26	4164

From Table 2, it is evident that increase in length and width of the cavity, reduces the frequency of the cavity resonance modes. The resulting coupling effect in the desired frequency range can be eliminated by either reducing the length of the cavity or changing the excitation at the frequency region, where no resonance modes occur. The comparison of the theoretical and eigen analysis for the unassembled and assembled cavities is shown in Table 3 for two different package geometries having same length which is determined by the physical dimensions of the components.

Both the package geometries have exhibited the frequency

components at 5.29 and 5.33 GHz with very high quality factors during eigen analysis of the assembled cavity. Although these frequencies are falling in the pass band, these have negligible coupling contribution due to higher Q factor.

4.2. Selection of Package Material

The effect of package material is analyzed to see its impact on the resonance modes. Here, space qualified package materials like Aluminium Alloy (6061-T6), Nickel, Magnesium and Kovar are considered for the eigen and driven solution of the unassembled cavity. The analysis results based on different materials for the same cavity dimensions are shown in Table 4 and Figure 5 respectively.

The results show that the resonant Mode_2 is closely matching

Table 4. Microwave enclosure effect based on package material.

Effective Modes	Materials	Eigen Freq. (GHz)	Quality factor	Driven Freq. (GHz)	Coupling (dB)
Mode_1	Al6061-T6	6.03	675307	5.86	−84.38
Mode_2		7.26	330376	7.26	−47.78
Mode_1	Mg	6.03	675714	5.88	−79.02
Mode_2		7.26	545008	7.26	−49.61
Mode_1	Ni	6.02	391.6	5.15	−104.00
Mode_2		7.24	436.53	7.26	−64.96
Mode_1	Kover	6.03	754375	5.88	−85.00
Mode_2		7.25	603691	7.26	−44.35

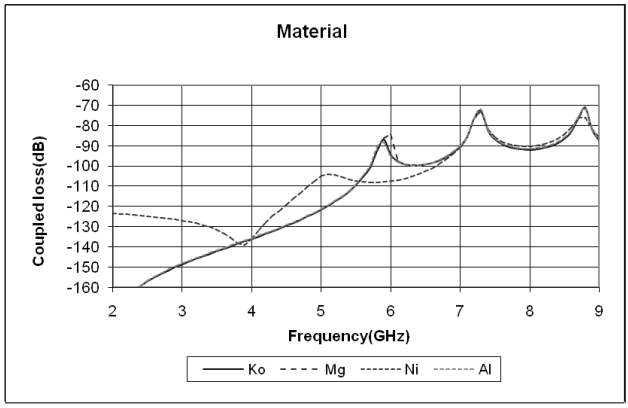

Figure 5. Material dependent coupling effect.

for both cases but frequency of Mode_1 differs slightly. But both resonant modes show high Q factor and hence the coupling contribution is minimum.

4.3. Selection of Absorber

In post design mitigation technique, the absorber is placed on the inner surface of the cover as shown in Figure 6 and the analysis has been carried out for different broadband absorbers. The properties of the absorbers are shown in Table 5 and the damping effect of the broadband absorbers is shown in Figure 7.

The broadband magnetically loaded microwave absorbers of types GDS, FDS and MFS of Emersion & Cuming are made of silicon that converts electromagnetic energy into heat through magnetic reorientation of iron particles. These absorbers have a high magnetic loss tangent and not suitable for the wide band amplifier, as it

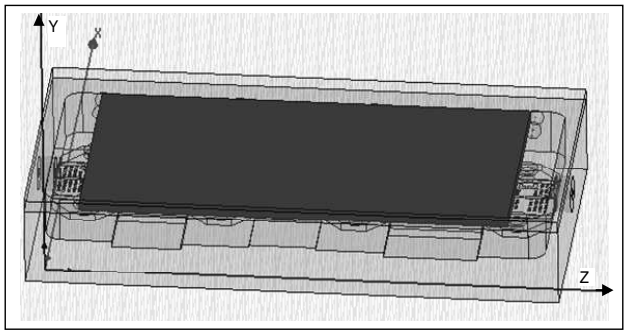

Figure 6. Microwave absorber study.

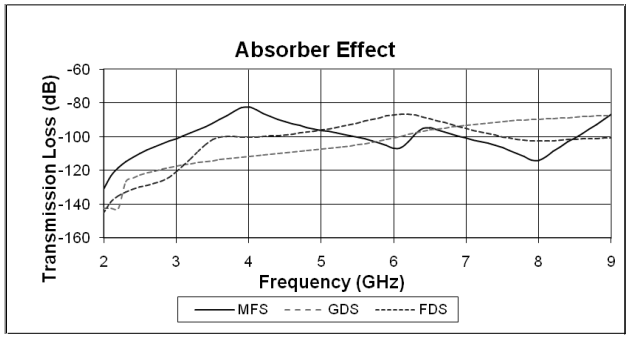

Figure 7. Damping effect of the absorbers.

can dampen the signal at frequency of interest. These materials have impedance equal to free space and do not reflect radiation at a normal incidence angle. The frequency selective, resonance type, microwave absorber should be used as per the mode to be attenuated without affecting the performance of microwave power amplifier. The microwave resonant absorber used here is SF-5, which is a thin, flexible, flat sheet, with out-gassing properties of Total Mass Loss (TML) < 0.1 and Collected Volatile Condensable Material (CVCM) < 0.06. The use of this absorber can cause RF suppression at 5 GHz at different degree based on angle of incidence. At 0° incident angle, it can reflect more than 35 dB. Subsequently the phase and magnitude of the eigen mode electric field pattern of the resonant mode 3 (5.17 GHz) as per Table 1,

Table 5. Properties of microwave absorbers.

Absorber Type	Relative permittivity	Dielectric Loss Tangent	Relative permeability	Magnetic loss Tangent
FDS	8.9	0.07	1.7	0.80
GDS	20.0	0.67	3.5	0.40
MFS	9.9	0.06	1.9	0.13

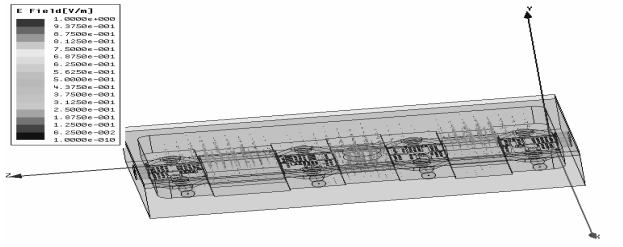

Figure 8. Phase of electric field.

Figure 9. Magnitude of electric field.

are shown in Figures 8 and 9. The mode at 5.2 GHz when excited by the radiation sources shows worst coupling of −12 dBc, as per driven solution of the assembled package. By using absorber on the total inner surface of the cover, the unwanted emission can be suppressed however it affects the performance in the desired frequency band because of its broadband nature. To avoid the use of absorber inside the whole cover, selective absorbers at specific locations are used, where magnitude of electric field is maximum.

5. DESIGN VALIDATION

To design a microwave power amplifier, first individual stages are designed at the frequency 5.35 GHz with 250 MHz bandwidth. During the design phase of matching circuits of the power amplifier, different methodologies are implemented to reduce the undesired emission. Measures include avoiding sharp corners in the MIC layout; using decoupling capacitor in the main transmission path of the microwave circuit and RF bypass capacitors for power supply lines. Each individual amplifier stage is made stable over the entire frequency range of the device. If the active device is not unconditionally stable, it is made stable by using resistive loading, preferably gate loading. Subsequently, integrated amplifier is designed and optimized by taking the housing effects in consideration. As the microwave medium power amplifier, under pulsed condition gives rise to unwanted emissions, this in turn may affect other subsystems in proximity due to EM radiation.

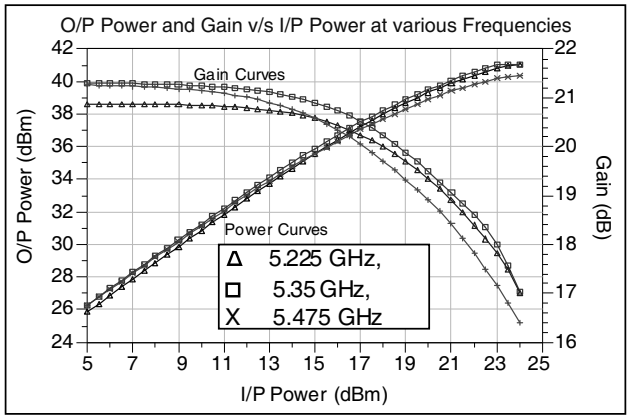

Figure 10. Simulated transfer characteristics and gain of microwave amplifier.

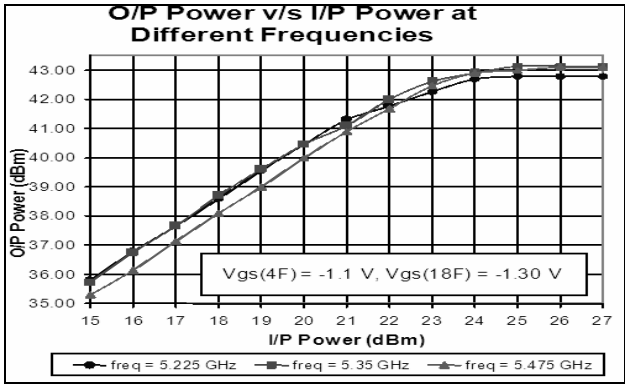

Figure 11. Measured transfer characteristics of microwave amplifier.

To improve the EMI/EMC performance, it is essential to take care of all the unwanted emissions from the pulsed Electronic Power Conditioner (EPC). EPC provides required drain and gate supplies with proper sequencing to suppress the conducted emission below the MIL-461E standards. All the critical requirements such as switching of power devices, transient suppression, surge protection etc. are taken care of while designing the Electronic Power Conditioner circuit [15]. The simulation and measured test results of the integrated amplifier are shown in Figures 10 & 11, which show compliance to the design requirement of output power ($P_{2\,dB}$) of more than of 12 watt for 22.5 dBm input power. During the EMI/EMC testing, the radiated susceptibility test is carried out for the radiation level of 5 V/m field strength in both horizontal and vertical polarizations. The radiated susceptibility and emission results are shown in Table 6 and Table 7 respectively. The photographs of the two amplifiers with different package dimensions, which are designed to validate the electrical design and EMI/EMC performance, are shown in Figure 12.

6. DISCUSSION

Study has been carried out to examine the effect of enclosures on the performance of the power amplifier at C-Band. It has been seen that though the un-assembled cavity does not exhibit any frequency components within the desired frequency band, the assembled structure shows several frequency components inside as well as outside the desired frequency band. The worst coupling (−12 dBc) appears at the 5.17 GHz frequency. The use of absorber under the

Table 6. Radiated susceptibility test RS-103.

Radiated Field		Spurious in dBc			
		Vertical Polarization		Horizontal Polarization	
Freq. (GHz)	Level (V/m)	Freq. (GHz)	Amplitude (dBc)	Freq. (GHz)	Amplitude (dBc)
2.2	5	2.2	< -100	2.2	< -100
4.5	5	4.5	< -100	4.5	< -100
5.225	5	5.225	-65.3	5.225	< -70
5.335	5	5.335	-69.7	5.335	< -70
5.475	5	5.475	-65.4	5.475	< -70
8.2	5	8.2	-100	8.2	< -100
8.4	5	8.4	-100	8.4	-100
8.6	5	8.6	-100	8.6	< -100

Table 7. Radiated emission test (RE-102).

Frequency and polarization		MIL STD 461E specification (dBμV/m)	Freq. of worst case RE (MHz)	Worst case RE (dBμV/m)
10 kHz TO 30 MHz		24.0	14.31	74.6
30 MHz TO 200 MHz	V	24.0	30.86	51.0
	H	24.0	42.29	31.8
1 GHz TO 20 GHz	V	58.5	5350	44.2
	H	58.5	5350	37.0

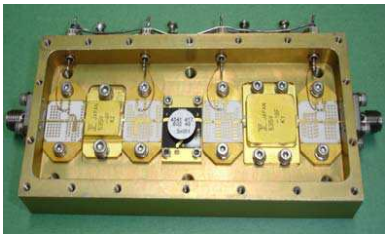

(95.2 mm x 40 mm x 12 mm)

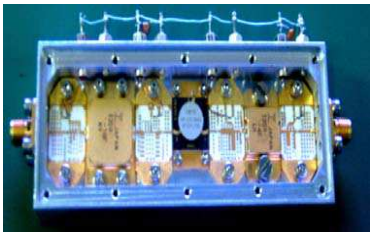

(95.2 mm x 29.8 mm x 12 mm)

Figure 12. Photograph of microwave amplifiers of different package geometry.

cover removes the unwanted emission however it affects the amplifier response in the desired frequency band. Instead, the absorbers can be used only at selected locations. The magnitude and phase of electric field for the worst coupled resonance modes are shown in Figure 8 and Figure 9, which provides the location of the maximum magnitude of the electric field. The other mitigation techniques like change of material or the change of cavity structure are also evaluated for the resonance free microwave amplifier performance.

7. CONCLUSION

The analytical solution of the rectangular package provides quick estimate of the resonance frequencies. The detailed package design and analysis is carried out for un-assembled cavity for three different packages with dimensions:

95.2 mm (length) × 40 mm (width) × 12 mm (height)
95.2 mm (length) × 45 mm (width) × 12 mm (height)
95.2 mm (length) × 29.8 mm (width) × 12 mm (height)

From Table 1 and Table 3, it is clear that the unassembled packages are not showing any dominating coupling components within the desired frequency range of the amplifier, because of high Q factors. On the contrary, the assembled structure shows number of resonance modes at different frequencies for the same packages. The dominant frequency components are 5.17 GHz, 5.2 GHz (from Table 1) and 5.29 GHz, 5.33 GHz (From Table 3), which are within the frequency band of amplifier. The contribution at these frequencies is negligible because of high quality factor. To make the design more robust, space grade absorbers are used as a post design mitigation technique to have resonance free stable microwave amplifier. Albeit broad band absorbers are used to suppress the unwanted resonance modes, these absorbers have the damping effect in the desired frequency band also. Hence resonant absorbers used at selected locations which are finalized based on the magnitude and phase of electric field for the worst coupled resonance modes. From the study of package material, it is clear that all the space qualified materials mentioned earlier, are suitable for microwave amplifier application because of low coupling contribution. But considering the physical properties of all the materials, it is clear that 'Mg' package will be lighter, but from the thermal conductivity and ease of machining point of view, aluminium with Ni plating will be the best package material for space applications. The overall performance of the amplifier designed has shown very close agreement with the simulated results.

ACKNOWLEDGMENT

The authors are thankful to the MIC facility, workshop, mechanical package designer and MSTD designers for their kind cooperation. We would also like to thank Shri D. R. M. Samudraiah, Deputy Director, SEDA for reviewing the paper and giving valuable suggestions. We are also very grateful to Dr. R. R. Navalgund, Director, Space Applications Centre for motivating us to write this paper and allowing us to publish it. The authors would also like to thank the reviewers and editors for their advice and suggestions.

REFERENCES

1. Dhar, J., S. K. Garg, R. K. Arora, and S. S. Rana, "Nonlinear model based power amplifier," *IEEE Applied Electromagnetics Conference*, 1–4, 2009.
2. Yook, J. G., L. P. B. Katehi, R. N. Simons, and K. A. Shalkhauser, "Experimental and theoretical study of parasitic leakage/resonance in a K/Ka-band MMIC package," *IEEE Transactions on Microwave Theory and Techniques*, Vol. 44, No. 12, Dec. 1996.
3. Decker, D. R., H. M. Olson, R. Tatikola, R. Gutierrez, and N. R. Mysoor, "Multichip MMIC package for X and Ka bands," *IEEE Tansactions on Components, Packaging and Manufacturing Technology*, Part B, Vol. 20, No. 1, Feb. 1997.
4. Chen, H. and Y. Zhang, "A synthetic design of eliminating crosstalk within MLTS," *Progress In Electromagnetics Research*, Vol. 76, 211–221, 2007.
5. Xiao, F. and Y. Kami, "Modeling and analysis of crosstalk between differential lines in high-speed interconnects," *PIERS Online*, Vol. 3, No. 8, 1293–1297, 2007.
6. Bernadi, P., R. Cicchetti, G. Pelosi, A. Reatti, S. Selleri, and M. Tatini, "An equivalent circuit for EMI prediction in printed circuit boards featuring a straight-to-bent microstrip line coupling," *Progress In Electromagnetics Research B*, Vol. 5, 107–118, 2008.
7. Nie, X. C., N. Yuan, L. W. Li, and Y. B. Gan, "Accurate modeling of monopole antennas in shielded enclosures with apertures," *Progress In Electromagnetics Research*, Vol. 79, 251–262, 2008.
8. Lei, J.-Z., C.-H. Liang, and Y. Zhang, "Study on shielding effectiveness of metallic cavities with apertures by combining

parallel FDTD method of windowing technique," *Progress In Electromagnetics Research*, Vol. 74, 82–112, 2007.

9. Bahadorzadeh, M. and A. R. Attari, "Improving the shielding effectiveness of a rectangular metallic enclosure with aperture by using extra shielding wall," *Progress In Electromagnetics Research Letters*, Vol. 1, 45–50, 2008.
10. Robertson, J., E. A. Parker, B. Sanz-Izquierdo, and J. C. Batchelor, "Electromagnetic coupling through arbitrary apertures in parallel conducting planes," *Progress In Electromagnetics Research B*, Vol. 8, 29–42, 2008.
11. Hattori, H. T., "Fractal like square lattices of air holes," *Progress In Electromagnetics Research Letters*, Vol. 4, 9–16, 2008.
12. Maab, H. and Q. A. Naqvi, "Fractional rectangular cavity resonator," *Progress In Electromagnetics Research B*, Vol. 9, 69–82, 2008.
13. Dhar, J., S. K. Garg, R. Singhal, R. K. Arora, and S. S. Rana, "Non-linear design, package analysis and thermal design of C-band CW power amplifier," *Proc. of International Conference on Computers and Devices for Communication (CODEC-06)*, Institute of Radiophysics and Electronics, University of Calcutta, Dec. 18–20, 2006.
14. *Ansoft High Frequency Structure Simulator*, Version 10, User's Manual.
15. Dhar, J., S. K. Garg, R. K. Arora, and S. S. Rana, "Performance enhancement of pulsed solid state power amplifier using drain modulation over gate modulation," *International Symposium on Signals, Circuits and Systems*, 1–4, Jul. 9–10, 2009.